Catalytic Effects of Subsurface Carbon in the Chemisorption of Hydrogen on a Mg(0001) Surface: an Ab-initio Study

A. J. Du,[†,‡] Sean C. Smith,*[,†,‡] X. D. Yao,[‡,§] and G. Q. Lu[‡]

Centre for Computational Molecular Science, Chemistry Building, The University of Queensland, QLD 4072, Brisbane, Australia, ARC Centre for Functional Nanomaterial, School of Engineering, The University of Queensland, QLD 4072, Brisbane, Australia, and School of Engineering, James Cook University, Townsville, QLD 4811, Australia

Received: October 19, 2005; In Final Form: December 5, 2005

Ab initio density functional theory (DFT) calculations are performed to explore possible catalytic effects on the dissociative chemisorption of hydrogen on a Mg(0001) surface when carbon is incorporated into Mg materials. The computational results imply that a C atom located initially on a Mg(0001) surface can migrate into the subsurface and occupy an fcc interstitial site, with charge transfer to the C atom from neighboring Mg atoms. The effect of subsurface C on the dissociation of H_2 on the Mg(0001) surface is found to be relatively marginal: a perfect sublayer of interstitial C is calculated to lower the barrier by 0.16 eV compared with that on a pure Mg(0001) surface. Further calculations reveal, however, that sublayer C may have a significant effect in enhancing the diffusion of atomic hydrogen into the sublayers through fcc channels. This contributes new physical understanding toward rationalizing the experimentally observed improvement in absorption kinetics of H_2 when graphite or single walled carbon nanotubes (SWCNT) are introduced into the Mg powder during ball milling.

Introduction

Among the metal hydrides under study as possible hydrogen storage media, magnesium hydride is one of the most promising candidates in the automotive industry due to its very high capacity in the stoichiometric limit (7.6 wt %) and low cost.[1−3] Unfortunately, its application is hindered by the fact that slow kinetics necessitates relatively high temperatures for hydrogenation and dehydrogenation. One of the possible reasons is that the hydrogen molecules do not readily dissociate on the Mg surface.[4,5] Experimentally, many studies have been devoted to the catalytic effect on hydrogen adsorption of mixing transition metals into the Mg powder by mechanical milling.[6−8] The transitional metal−Mg interfaces are thought to act as a catalyst to accelerate hydrogen sorption kinetics, in particular the dissociative chemisorption of molecular hydrogen into adsorbed atoms.[9,10] Apart from metallic alloying, some nonmetallic elements such as graphitic carbon have been noted to facilitate the activation process of Mg and improve the absorption kinetics of H_2.[11−15] The role of graphitic carbon has been thought to involve inhibition of formation of a new oxide layer on the Mg powder surface.[15] More recently, a very fast hydrogenation was also observed in our group by using single walled carbon nanotubes (SWCNTs) in ball milling experiments. These experiments are carried out in the absence of oxygen, suggesting a possible catalytic mechanism for C in addition to its possible role in preventing oxide layer formation. The catalytic mechanism that may operate when graphite or SWCNTs are incorporated as additives still remains unclear.

Density functional theory (DFT) calculations have shown considerable predictive power for the analysis of catalytic mechanisms.[16] Much insight can be gained for the process of designing alloy catalysts just from first principle simulations.[17−18] To date, only relatively few calculations of the dissociative chemisorption of H_2 onto a clean magnesium surface have been performed.[19−21] The energetically favored pathway and the activation barrier have been reported for this process. To clarify the recent experimental results and improve the hydrogenation performance of magnesium-based materials, it is very important to investigate the role of carbon in the dissociation of H_2 on Mg(0001) surfaces and the diffusion of atomic H from Mg surface into the subsurface.

In this paper, the effects of incorporated carbon atoms on the dissociation of H_2 on a Mg(0001) surface and on the diffusion of the atomic H into subsurface layers are studied by ab initio DFT calculations. The surface C/Mg architecture under vacuum is studied first. We found that surface C atoms can preferentially migrate into the subsurface layer and occupy an fcc interstitial site. Subsequently, we utilize the nudged elastic band (NEB) method to compute the minimum energy pathway (MEP) and dissociation barriers of H_2 on a clean Mg(0001) surface without and with an ideal monolayer of subsurface C atoms. We also present the results of structural relaxation/equilibration calculations for two dissociated hydrogen atoms on Mg(0001) surfaces with incorporation of a limited number of subsurface C atoms (six). These latter results are suggestive of a possible role for C in facilitating diffusion of atomic hydrogen down fcc channels into the subsurface. In the next section we outline our computational method. Section III presents our calculated results and discussion, and the last section is devoted to conclusions.

Computational Methods

The DFT calculations were performed using the plane-wave basis VASP code[22,23] implementing the generalized gradient approximation (GGA) of PBE exchange correlation functional.[24] An all-electron description, the projector augmented wave method (PAW),[25,26] is used to describe the electron−ion

* Corresponding author: Fax: 617-33654623, E-mail: s.smith@uq.edu.au.
† Centre for Computational Molecular Science, The University of Queensland.
‡ School of Engineering, The University of Queensland.
§ School of Engineering, James Cook University.

10.1021/jp055972d CCC: $33.50
Published on Web 01/06/2006

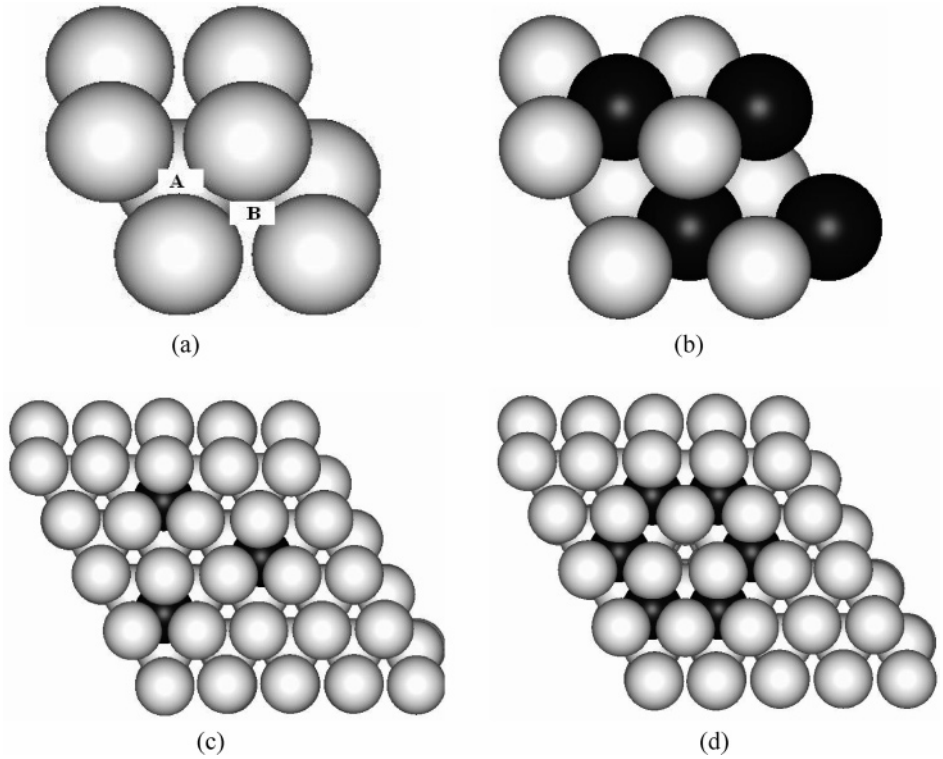

Figure 1. Models used in our calculation. (a) A (2 × 2) Mg(0001) surface. A and B represent hcp and fcc sites, respectively. (b) Top view of the relaxed (2 × 2) Mg(0001) surface with an ideal monolayer subsurface C atoms. (c) Top view of the relaxed equilibrium configuration for a (5 × 5) Mg(0001) surface with three subsurface carbon atoms. (d) The same as (c) but for a (5 × 5) Mg(0001) surface with six subsurface carbon atoms.

interaction. The cutoff energy for plane waves is chosen to be 500 eV for a very accurate energy calculation. As shown in Figure 1a and 1b, Mg(0001) surfaces without and with an ideal monolayer C atoms at subsurface are modeled by using a (2 × 2) surface unit cell with five layers of Mg. A (4 × 4 × 1) Monkhost-Pack grid is used in the Brillouin-zone sampling.[27] For Mg(0001) surface with three or six C atoms at the subsurface, we chose a big (5 × 5) surface unit cell (see Figure 1d), and only the gamma point is used for this calculation. To determine dissociation barriers and MEP, the NEB method was used.[28−29] This method involves optimizing a chain of images that connect the reactant and product state. Each image is allowed to move only into the direction perpendicular to the hyper-tangent. Hence the energy is minimized in all directions except for the direction of the reaction path. A damped molecular dynamics was used to relax ions until the forces in each image are less than 0.02 eV/Å. The vacuum space is 16 Å, which is enough to guarantee a sufficient separation between periodic images.

Results and Discussions

To benchmark the computational methods, a set of preliminary calculations on the specific systems (Mg−C−H) have been performed. By using the ab initio PAW method, the lattice constants of bulk Mg and MgH_2 are calculated to be 3.191 Å and 4.510 Å, respectively, which are only 0.5% and 0.2% in error compared with the experimental value.[30,31] The bond length of a hydrogen molecule and a C_2 dimer in gas phase are found to be 0.75 Å and 1.28 Å, respectively. The binding energy and the vibration frequency of hydrogen molecules are 4.51 eV and 4375 cm^{-1}, respectively. These are collectively in good agreement with the experimental results.[32]

As a first step in exploring the possible role of incorporated carbon in facilitating the absorption of hydrogen, as studied experimentally recently,[11−15] the surface composition in vacuum space must be determined. A plausible reference configuration may be one full monolayer graphite sheet positioned on a Mg-(0001) surface. A single (4 × 4) graphite sheet and a (3 × 3) Mg(0001) surface unit cell with five layers of Mg slab are used to reduce the lattice mismatch (lattice constant are 2.44 Å for graphite and 3.191 Å for Mg). By performing geometry optimization, we found that the interaction between graphite sheet and Mg(0001) surface is a typical van der Waals (vdW) type with an equilibrium distance of 3.68 Å, as shown in Figure 2a. The binding energy is calculated to be only 0.30 eV without considering vdW correction to GGA.[33] While this type of dispersive interaction between graphitic or nanotube carbon and Mg is a plausible model for the initial state of the system prior to ball milling, it is important to note that experimentally no surface carbon is detected post ball milling, implying presumably that the carbon has been largely atomized and dispersed within the material.[34] On the basis of previous studies, the atomization energy of graphite and carbon nanotubes is known to be as high as 7.0 eV.[35,36] Mechanical ball milling is, however, a highly energetic process. Hence, it is not surprising that atomic carbon can be produced during ball milling by mixing small amounts of graphite (5%) into the Mg material. To study such configurations, we then deposited one C atom on either a top or a bridge site at a distance of 1.5 Å from the Mg(0001) surface and optimized the geometry. Surprisingly, the surface carbon atom was found in the relaxed configuration to have migrated into the subsurface layer, and finally it occupied a fcc site as shown in Figure 2b. The relaxation energy for the C atom deposited initially in this way is considerable (e.g., −4.5 eV for on-top deposition). The binding energy (E_b) for C incorporated into Mg subsurface is calculated by

$$E_b = E_{Mg(0001)+C} - E_{Mg(0001)} - E_C \quad (1)$$

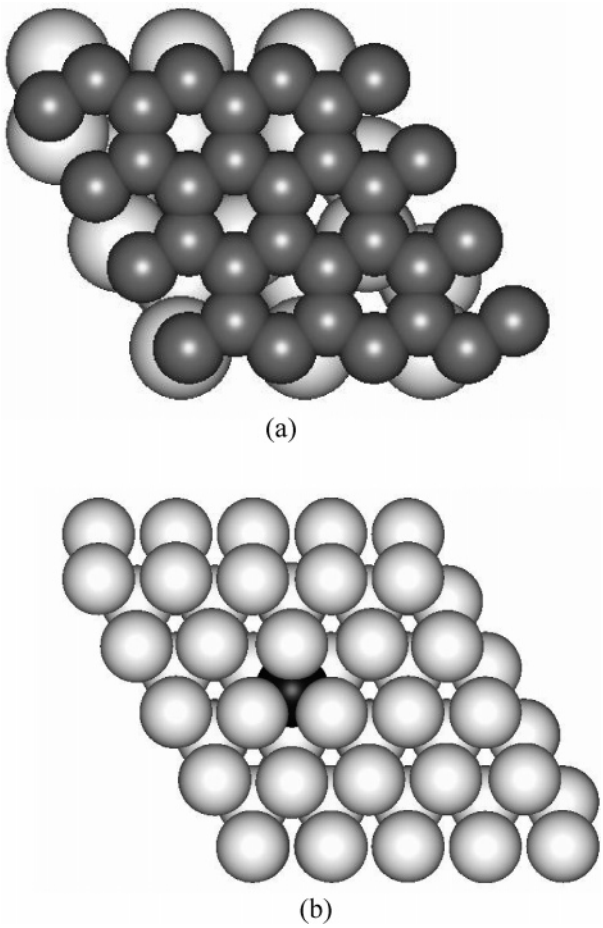

Figure 2. (a) Top view of the relaxed configuration for a (4 × 4) graphitic sheet on a (3 × 3) Mg(0001) surface. (b) Top view of the relaxed equilibrium configuration (i.e., subsurface fcc site occupancy) for one C atom deposited initially on a (5 × 5) Mg(0001) surface.

where $E_{Mg(0001)+C}$, $E_{Mg(0001)}$, and E_C represent the total energy of Mg(0001) surface with a subsurface carbon atom, clean Mg(0001) surface, and an isolated carbon atom. The E_b is calculated to be 7.16 eV, which implies sufficiently positive segregation energy to be required to move a solute atom from the bulk to the surface of the host metal.[17] In this case, subsurface carbon is the energetically preferred configuration. As reported in other works,[37] such configurations may vary with increasing coverage of surface carbon atoms. To explore this, geometry optimizations were then performed starting at several configurations with different coverage of surface carbon atoms. We found that all the surface C atoms can migrate into the subsurface when the coverage is less than 0.5. At high coverage ($\theta > 0.5$), some of C atoms prefer to stay on the Mg(0001) surface. To gain more insight for the equilibrium configuration containing a subsurface carbon, the valence charge electron density difference (ρ_{diff}) in vacuum space is analyzed by the following equation and plotted in Figure 3.

$$\rho_{diff} = \rho_{Mg(0001)+C} - \rho_{Mg(0001)} - \rho_C \qquad (2)$$

Here $\rho_{Mg(0001)+C}$, $\rho_{Mg(0001)}$, and ρ_C represent the valence charge density for Mg(0001) surface with a subsurface carbon atom, clean Mg(0001) surface, and a isolated carbon atom having the same position as the subsurface carbon. It can be seen clearly that there is charge accumulation on the subsurface C atom and charge depletion from neighboring Mg atoms. This indicates a significant charge transfer between them. Additionally, charge analysis was also performed for the equilibrium configuration

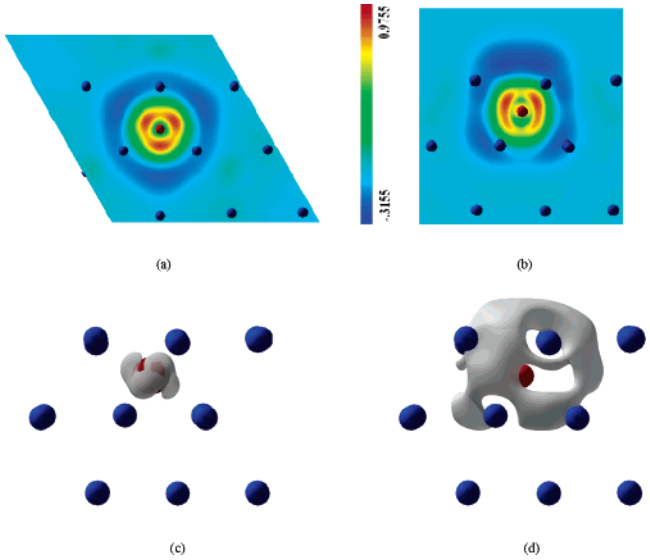

Figure 3. Contour plots of valence charge difference in (a) XOY plane and (b) XOZ plane containing subsurface C and neighboring Mg atoms. (c) and (d) are 3D iso-surface plots of valence electron charge density difference, which show charge accumulation (iso-value: 0.75 electron/Å^3) on subsurface C atom and charge depletion (iso-value: −0.15 electron/Å^3) from neighboring Mg atoms, respectively.

by voronoi partitioning.[38] The amount of charge transfer is about 1.0 electron from neighboring Mg atoms to the subsurface C atom.

Having established the energetically preferred configuration for a C atom on a Mg(0001) surface, the ensuing question is whether the subsurface C atom will affect the dissociative chemisorption of H_2 on the Mg(0001) surface. To explore this, a series of NEB calculations were performed to obtain the MEP and the activated barrier for the dissociation of H_2 on a Mg(0001) surface without and with an ideal monolayer of subsurface C atoms (see Figure 1a and Figure 1b). Based on the previous studies of H_2 dissociation on a pure Mg(0001) surface,[19−21] the energetically favored pathway involves H_2 dissociating at a bridge site and the nascent atoms moving into A (a hcp site) and B (a fcc site) (see Figure 1a). The dissociated H atom on the hcp site will then quickly diffuse onto another neighboring fcc site. Despite the fact that two fcc sites are energetically preferred, the final state (FS) in our calculation is chosen to be a "meta" configuration, in which the hydrogen atoms are positioned on the A and B sites (see Figure 1a), respectively. This should not affect the activation barrier for H_2 dissociation on the Mg surface and simplifies our NEB calculation. We set one hydrogen molecule onto the relaxed Mg (0001) surface at a distance of 5 Å as the initial state (IS). Chains of images linking the IS and FS are built and minimized according to the appropriate effective force acting on each image. All the NEB calculations have been made in exactly the same technical conditions, i.e., the same cutoff and supercell dimensions in order to get an effective cancellation of errors. The energy profiles for H_2 dissociation on each surface, as revealed by our NEB calculations are reported in Figure 4. Solid (with square) and dash (with triangle) lines correspond to the dissociation of H_2 on Mg(0001) surface without and with an ideal monolayer C atoms at subsurface, respectively. It was found that the energetically favored pathway is almost the same for both surfaces. However, the activation barrier for H_2 dissociation on Mg(0001) with an ideal subsurface monolayer C atoms is 0.16 eV smaller than that on pure Mg(0001) surface.

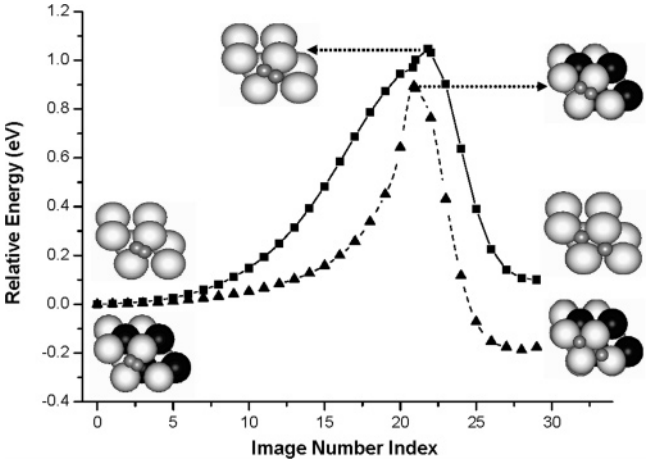

Figure 4. The energy profiles for the dissociation of a H2 molecule on a Mg(0001) surface: with (▲) and without (■) an ideal subsurface monolayer of C atoms. The horizontal axis is the image number. Three special configurations (IS, TS, and FS) along the MEPs are also given. The large white, large black, and small gray balls represent Mg, C, and H atoms, respectively.

TABLE 1: Calculated Vibrational Frequencies and Zero-Point Energy Correction of Molecular and Atomic Hydrogen for the IS, TS, and FS in the Dissociation of H_2 on Mg(0001) Surface without and with an Ideal Monolayer Subsurface Carbon Atoms (Im indicates imaginary frequency of reaction coordinate)

	vibration frequency, ω(cm^{-1})			(1/2) $\sum_i \omega_i$(meV)
H_2		4375		265.0200
TS (without C)	Im	878.326097	873.365809	214.4125
	575.458113	769.638495	361.969821	
TS (with C)	Im	973.569939	829.632440	203.5831
	745.609388	456.603622	278.593880	
FS (without C)	1187.157124	894.288690	665.543835	302.8940
	934.689493	767.845684	468.760097	
FS (with C)	876.234287	724.911560	1084.510527	282.8694
	594.871611	345.565170	936.897531	

Zero-point vibrations of hydrogen are known to be important for the prediction of absolute energetics, hence we have performed vibrational frequency analysis based on the harmonic oscillator approximation to explore the effects on the dissociation barrier of H_2. Table 1 presents the calculated vibrational frequencies and zero-point energy (ZPE) correction of molecular and atomic hydrogen for the IS, TS, and FS in the dissociation of H_2 on Mg(0001) surface, without and with an ideal monolayer subsurface carbon atoms. Here Im indicates the imaginary frequency of the reaction coordinate. Apparently, the total change in the ZPE between IS and TS are seen to be as high as 0.051 eV and thus has a significant effect on the effective activation barrier. However, the *difference* between the H_2 dissociation on Mg surface with and without subsurface C atoms is only 0.011 eV. This is due to the fact that the reaction paths are very similar in each case, as shown in Figure 4. Hence, our conclusions about the effect of subsurface carbon on the surface dissociation of H_2 are not altered by the inclusion of the ZPE correction.

As pointed out in the work of Norskov,[39] the barriers to chemisorption or dissociation come from the initial dominance of "kinetic energy repulsion", namely the Pauli effect at work. The position where H_2 begins to dissociate on a Mg(0001) surface with an ideal monolayer of subsurface carbon atoms is located at a distance of 1.4 Å from the top of surface, which is 0.38 Å higher than for the pure Mg(0001) surface. So the decreased barrier could be understood in terms of the charge transfer from surface Mg atoms to subsurface C atoms alluded to above (see Figure 3) and thus the possibly decreased Pauli repulsion of the adsorbate orbitals with the s,p metal state. Additionally, we have also studied the binding energy of H atom on hcp and fcc sites for both surfaces. We found that the binding energy increased somewhat (by 0.32 eV for hcp and by 0.27 eV for fcc sites) on the Mg(0001) surface with an ideal subsurface monolayer of C atoms. Generally, strong binding of H would be expected to imply a lower activation energy barrier for the dissociative chemisorption,[40−42] except for near-surface transition metal alloys with a *d* metal state.[17]

To further understand the dissociation mechanism of H_2 on both surfaces, the density of states (DOS) corresponding to IS, TS, and FS projected onto the two H atoms are plotted in Figure 5. The bonding (σ_g) and antibonding (σ_u*) of hydrogen molecule can be seen clearly in the IS as shown in Figure 5a and 5d. As the dissociation proceeds, σ_u* will be shifted down to lower energy across the Fermi level and the main peaks of σ_g are reduced. The H−H interaction is weakened and H-substrate interaction becomes stronger. The σ_g and σ_u* splitting decreases, and finally the two states mix together below the Fermi level (see FS in Figure 5c and 5f). In the TS, the σ_g bonding state for H_2 on Mg(0001) surface with an ideal monolayer subsurface carbon atoms is closer to the Fermi level compared with pure Mg(0001) surface (see TS in Figure 5b and 5e).

The hydrogenation of magnesium involves dissociation of molecular hydrogen on the Mg surface in the first step, followed subsequently by diffusion of the dissociated H atoms into the subsurface fcc sites through the fcc channels,[20,43] which are thought to be the most plausible diffusion pathway. Transparently, it would be difficult for the dissociated H atoms to diffuse subsequently into the Mg bulk if subsurface C atoms occupied all the fcc channels (See Figure 1b). Hence, the model with an ideal subsurface monolayer of C atoms, while revealing, is not entirely satisfactory. To explore the possible effect of sublayer C atoms on the diffusion of the dissociated H atom, a more realistic model involving a Mg(0001) surface with a sparse or incomplete subsurface layer of C atoms is needed (see Figure 1c and Figure 1d). As a step toward exploring these possibilities, we optimize the geometry of a system (Figure 6a) where two H atoms are positioned initially on A and B sites on a Mg-(0001) surface which incorporates six subsurface C atoms centered around a fcc site within a (5 × 5) Mg(0001) surface unit cell. Figure 6b shows the equilibrium configuration obtained with the conjugate gradient method. The H atom initially located on the surface fcc site has relaxed into occupation of the subsurface fcc site underneath, while the H atom initially located on the surface hcp site has moved onto the previously occupied surface fcc site. This provides a strong hint that subsurface C atoms may also affect the diffusion of H atoms on the surface and into the subsurface. We note that the barrier for migration of atomic hydrogen from the surface fcc site on Mg(0001) into the first sublayer has been calculated to be ca. 0.5 eV.[43] The result of the present conjugate gradient relaxation calculation implies that this migration can occur in the presence of subsurface carbon with only a very small barrier, if any at all. Thus, it is apparent that subsurface C atoms can not only facilitate advantageous positioning of H atoms on the surface after dissociation, but can also promote a "funneling" effect, facilitating diffusion of atomic H into the subsurface by lowering the activation barriers to transport down the encircled fcc channels. Full NEB calculations of the barriers for surface diffusion and migration into the sublayer in the presence of subsurface C are reserved for a separate work.[44] It suffices to

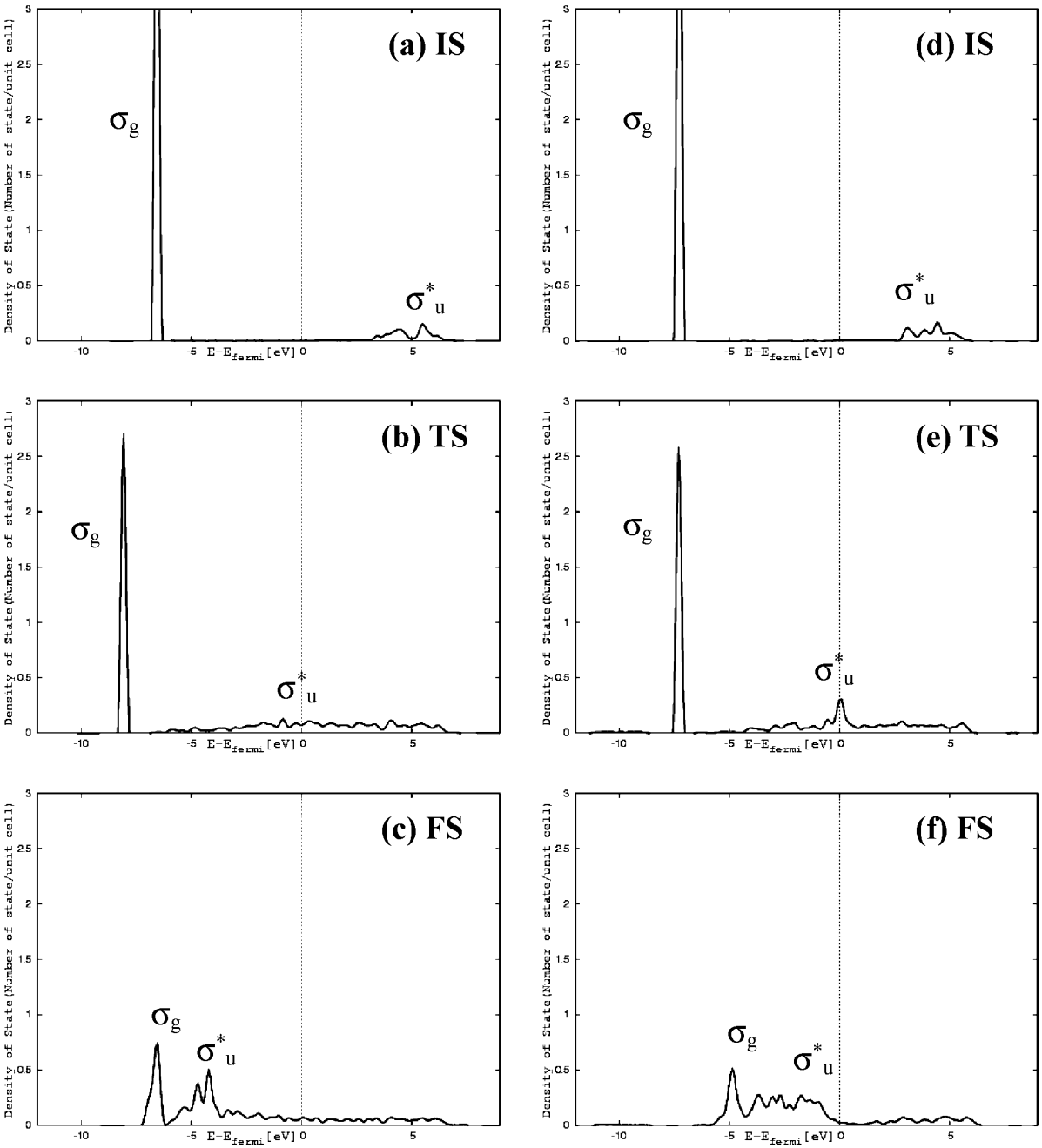

Figure 5. The density of states (DOS) corresponding to IS, TS, and FS are projected onto the two H atoms. (a), (b), and (c) are for pure Mg(0001) surfaces; (d), (e), and (f) are for a Mg(0001) surfaces with an ideal layer of subsurface carbon atoms. The vertical dotted line represents the Fermi Level.

say in the present context that the postulated lowering of the barriers in the presence of subsurface C is indeed verified.

Conclusions

In summary, ab initio DFT calculations were performed to study the role of incorporated C atoms in facilitating the dissociation of H_2 and the diffusion of atomic H on Mg(0001) surfaces. We find that a C atom on a Mg(0001) surface can undergo facile migration into the subsurface layer and occupy an fcc interstitial site. Charge will be transferred to the subsurface C atom from the neighboring Mg atoms. This is an important finding which helps to explain the experimental fact that no elemental surface carbon is observed post ball milling.[34]

The dissociation barrier of H_2 on a Mg(0001) surface with an ideal monolayer of subsurface C atoms is calculated to be 0.16 eV smaller than that on a pure Mg(0001) surface (1.05 eV). We note that we have also carried out the NEB calculations for dissociation of H_2 on Mg(0001) with a sparse arrangement of subsurface carbon (three C atoms in the sublayer, see Figure 1c). The resultant MEP potential profile is quite similar to that of Figure 4, and hence we have not shown these data separately. The barrier to dissociation in this case was calculated to be just 0.255 eV lower that that for dissociation of H_2 on a pure Mg(0001) surface. These findings imply that the effect of subsurface C on the initial dissociation of molecular hydrogen on the Mg (0001) surface is relatively marginal.

The results for the specific models investigated in this work do however clearly indicate that diffusion of H atoms into the subsurface can be assisted by the presence of subsurface carbon, a conclusion supported further by extended NEB calculations

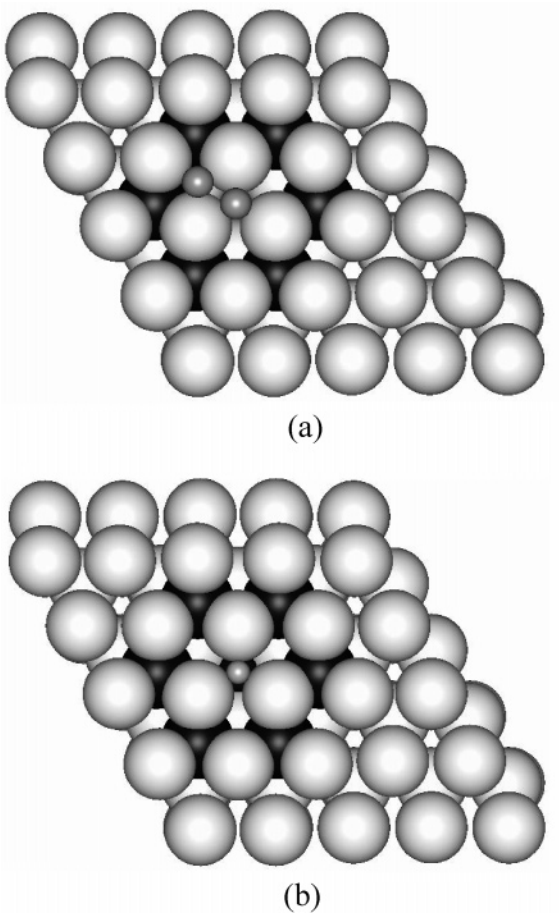

Figure 6. Prescribed initial and relaxed final configurations for a system of two H atoms interacting with a Mg(0001) surface incorporating six subsurface C atoms centered around an unoccupied fcc site. (a) The initial configuration for geometry optimization. (b) The final configuration obtained after full relaxation. The large white, large black, and small gray balls represent Mg, C, and H, respectively. For Figure 6b, the small black ball (center, sublayer) represents the second hydrogen atom that has migrated to the sublayer.

published separately.[44] Taken collectively, our findings in this study therefore suggest that the catalytic role of incorporated carbon is unlikely to impact the surface dissociaton, but rather will facilitate the mobility of atomic hydrogen in the Mg material. Effective materials for hydrogen storage currently under investigation via ball milling experiments often contain a coctail of additives in low percentages to optimize the kinetics, the capacity, and the reversibility of hydrogen absorption. The present study will contribute to an understanding of the catalytic roles being played by carbon additives in such complex nanocomposite materials.

Acknowledgment. We acknowledge generous grants of high-performance computer time from both the Computational Molecular Science cluster computing facility at The University of Queensland and the Australian Partnership for Advanced Computing (APAC) National Facility. The authors also greatly appreciate the financial support by Australian Research Council through the ARC Centre for Functional Nanomaterials.

Supporting Information Available: Structures for a (2×2) Mg(0001) surface with one monolayer subsurface carbon atoms (Figure 1b), (5×5) Mg(0001) surfaces with three and six subsurface carbon atoms (Figure 1c and 1d), and prescribed initial and relaxed final configurations for a system of two H atoms interacting with a Mg(0001) surface incorporating six subsurface C atoms centered around an unoccupied fcc site (Figure 6a and 6b). This material is available free of charge via the Internet at http://pubs.acs.org.

References and Notes

(1) Schwarz, R. B *MRS Bull.* **1999**, *24*, 40.
(2) Schlapbach, L.; Zuttel, A. *Nature* **2001**, *414*, 23.
(3) Liang, G.; Huot, J.; Van Neste, A.; Schulz, R. *J. Alloys Compd.* **1999**, *292*, 247.
(4) Zaluska, A.; Zaluski, L.; Strom-Olsen, J. O. *Appl. Phys. A: Mater. Sci. Process.* **2001**, *72*, 157.
(5) Von Zeppelin, F.; Reule, H.; Hirscher, M. *J. Alloys Compd.* **2002**, *330*−*332*, 723.
(6) Bobet, J. L.; Chevalier, B.; Darriet, B. *J. Alloys Compd.* **2002**, *330*, 738.
(7) Rivoirard, S.; de Rango, P.; Fruchart, D.; Charbonnier, J.; Vempaire, D. *J. Alloys Compd.* **2003**, *356*−*357*, 622.
(8) Arico, A. S.; Bruce, P.; Scrosati, B.; Tarascon, J. M.; Van Schalkwijk, W. *Nature Mater.* **2005**, *4*, 366.
(9) Yavari, A. R.; de Castro, JFR.; Heunen, G.; Vaughan, G. *J. Alloys Compd.* **2003**, *353*, 246.
(10) Du, A. J.; Smith, S. C.; Yao, X. D.; Lu, G. Q. *J. Phys. Chem. B* **2005**, *109*, 18037.
(11) Bouaricha, S.; Dodelet, J. P.; Guay, D.; Huot, J.; Boily, S.; Schulz, R. *J. Alloys Compd.* **2000**, *307*, 226.
(12) Bouaricha, S.; Dodelet, J. P.; Guay, D.; Huot, J.; Schulz, R. *J. Alloys Compd.* **2001**, *325*, 245.
(13) Imamura, H.; Tabata, S.; Shigetomi, N.; Takesue, Y.; Sakata, Y. *J. Alloys Compd.* **2002**, *330*−*332*, 579.
(14) Imamura, H.; Tabata, S.; Takesue, Y.; Sakata, Y.; Kamazaki, S. *Int. J. Hydrogen Energy* **2000**, *25*, 837.
(15) Shang, C. X.; Guo, Z. X. *J. Power Source* **2004**, *129*, 73.
(16) Greeley, J.; Norskov, J. K.; Mavrikakis, M. *Annu. Rev. Phys. Chem.* **2002**, *53*, 319.
(17) Greeley, J.; Mavrikakis, M. *Nature Mater.* **2004**, *3*, 810.
(18) Vang, R. T.; Honkala, K.; Dahl, S.; Vestergaard, E. K.; Schnadt, J.; Egsgaard, E.; Clausen, B. S.; Norskov, J. K., Besenbacher, F. *Nature Mater.* **2005**, *4*, 160.
(19) Norskov, J. K.; Houmoller, A. M. *Phys. Rev. Lett.* **1981**, *46*, 257.
(20) Vegge, T. *Phys. Rev. B* **2004**, *70*, 035412.
(21) Bird, D. M.; Clarke, L. J.; Payne, M. C.; Stich, I. *Chem. Phys. Lett.* **1993**, *212*, 518.
(22) Kresse, G.; Furthmuller, J. *Comput. Mater. Sci* **1996**, *6*, 15.
(23) Kresse, G.; Furthmuller, J. *Phys. Rev. B* **1996**, *54*, 11169.
(24) Perdew, J. P.; Burke, K.; Ernzerhof, M. *Phys. Rev. Lett.* **1996**, *77*, 3865.
(25) Blochl, P. E. *Phys. Rev. B* **1994**, *50*, 17953.
(26) Kresse, G.; Joubert, D. *Phys. Rev. B* **1999**, *59*, 1758.
(27) Monkhorst, H. J.; Pack, J. D. *Phys. Rev. B* **1976**, *13*, 5188.
(28) Henkelman, J.; Jónsson, H. *J. Chem. Phys.* **2000**, *113*, 9978.
(29) Henkelman, J.; Uberuaga, B. P.; Jónsson, H. *J. Chem. Phys.* **2000**, *113*, 9901.
(30) Wyckoff, W. G. *Crystal structure*; Wiley Interscience: New York, 1963; Vol. 1.
(31) Bortz, M.; Bertheville, B.; Bottger, G.; Yvon, K. *J. Alloys Compd.* **1999**, *287*, L4.
(32) Lide, D. R. *CRC Handbook of Chemistry and Physics*; CRC Press: Boca Raton, 1995; p 1913.
(33) Du, A. J.; Smith, S. C. *Nanotechnology* **2005**, *16*, 2118.
(34) Yao, X. D.; Lu, G. Q.; Wu, C. Z.; Cheng, H. M.; Zou, J.; He, Y. *J Mater. Sci. Technol.*, in press.
(35) Brenner, D. W.; Shenderova, O. A.; Harrison, J. A.; Sturart, S. J.; Ni, B.; Sinnott, S. B. *J. Phys.: Condens. Matter* **2002**, *14*, 783.
(36) Yin, M. T.; Cohen, M. L. *Phys. Rev. B* **1984**, *29*, 6996.
(37) Christensen, A.; Ruban, A. V.; Stoltze, P.; Jacobsen, K. W.; Skriver, H. L.; Nørskov, J. K.; Besenbacher, F. *Phys. Rev. B* **1997**, *56*, 5822.
(38) Henkelman, G.; Arnaldsson, A.; Jónsson, H. *Comput. Mater. Sci.*, in press.
(39) Norskov, J. K.; Holloway, S.; Lang, N. D. *Surf. Sci.* **1984**, *137*, 65.
(40) Norskov, J. K *J. Catal.* **2002**, *209*, 275.
(41) Xu, Y.; Ruban, A. V.; Mavrikakis, M. *J. Am. Chem. Soc.* **2004**, *126*, 4717.
(42) Michaelides, A. *J. Am. Chem. Soc.* **2003**, *125*, 3704.
(43) Jacobson, N.; Tegner, B.; Schröder, E.; Hyldgaard, P.; Lundqvist, B. I. *Comput. Mater. Sci.* **2002**, *24*, 273.
(44) Du, A. J.; Smith, S. C.; Yao, X. D.; He, Y.; Lu, G. Q. *J. Phys. C: Conference Series*, in press.